

Controlled surface distribution and luminescence of $\text{YVO}_4:\text{Eu}^{3+}$ nanophosphor layers

A. F. Khan,¹ D. Haranath,^{1,a)} Ravishanker Yadav,¹ Sukhvir Singh,¹ S. Chawla,¹ and V. Dutta²

¹National Physical Laboratory, Council of Scientific and Industrial Research, Dr. K.S. Krishnan Road, New Delhi 110 012, India

²Centre for Energy Studies, Indian Institute of Technology Delhi, Hauz Khas, New Delhi 110016, India

(Received 11 June 2008; accepted 29 July 2008; published online 19 August 2008)

A method of dispersing $\text{YVO}_4:\text{Eu}$ quantum dots (QDs) as uniform two-dimensional (2D) layers with a high degree of homogeneity is presented. Annealing at 773 K resulted in coalescence of QDs to form nanoclusters with size of ~ 25 nm with an improved photoluminescence and $\sim 80\%$ transmittance at 800 nm. An efficient ${}^5D_0\text{-}{}^7F_2$ transition and lifetimes of ~ 1038 μs for the characteristic Eu^{3+} emission were observed. The absorption and emission peaks showed a slight blueshift, due to quantum-size effect, as compared to that for the bulk counterpart. Our method of 2D layer deposition is useful to enhance spectral response of the solar cells. © 2008 American Institute of Physics. [DOI: 10.1063/1.2973163]

Quantum dots (QDs) have attracted much attention due to their potential applications for many high performance devices,¹ viz., the Si-solar cell² and QD based light emitting diodes.³ Chemically synthesized^{4,5} QDs with precise size (< 5 nm) control and a suitable organic/inorganic cap are currently available for many practical applications.⁶ The QDs of phosphor materials could be even more interesting as they do not scatter light and show enhanced emission efficiencies⁷ and radiative lifetime shortening.⁸ The spatially distributed phosphor QDs can act as a thin layer having good optical transparency and high emission characteristics. Such a layer can be useful for increasing the power conversion efficiency of a solar cell. The objective of the present study is to fabricate highly transparent and luminescent two-dimensional (2D) layer using inorganic capped YVO_4 QDs that possess the advantages of quantum-size effect. Annealing treatments performed to the layers not only initiated the nanocluster formation but also provided a proper thermal encapsulation, adherence, and increased PL emission related efficiencies.

In utilizing nanoparticles for device technology one of the fundamental issues is how to distribute nanoparticles uniformly over a substrate with a precise control of particle density. In most of the studies, the self-assembly scheme has been employed using the chemical interaction between the nanoparticles and the substrate.⁹⁻¹¹ This method is effective in achieving a dense layer of nanoparticles. However, the control of the particle density is difficult at submonolayer regime. Moreover, special chemical treatments of the substrate surface are needed and the results are sensitive to local chemical environment with enhanced defect susceptibility.

In this letter, we demonstrate the fabrication of uniformly distributed sodium hexametaphosphate (SHMP) capped $\text{YVO}_4:\text{Eu}$ nanophosphor layer with controlled particle density using the conventional spin-coating method followed by annealing treatment.

It is well known that the OH^- groups show significant luminescence quenching behavior for most of the inorganic QDs.¹² Commonly, researchers synthesize $\text{YVO}_4:\text{Eu}$ nano-

phosphor by wet-chemical methods and protect the surface atoms by phosphate capping followed by redispersion in de-ionized water. This results in fully hydrated shell, and therefore, completes quenching of the photoluminescence (PL) by the surface atoms. Hence, the overall radiative efficiency goes down by many orders when compared to the bulk sample. To overcome this constraint we employed a nonhydrated phosphate dispersion of $\text{YVO}_4:\text{Eu}$ QDs and spin casted the films, resulting in substantial enhancement in luminescence intensities.

In a typical experiment, stoichiometric amounts of soluble salts of yttrium, vanadium, and europium were dissolved in aqueous media to which a mixture of NH_4OH and H_2O_2 in the volume ratio 3:1 was added. When the pH of the solution was adjusted to ~ 8.0 , ultrafine particles of $\text{YVO}_4:\text{Eu}$ precipitated out. The pale yellow body color of the precipitate confirmed the formation of $\text{YVO}_4:\text{Eu}$ QD agglomerates, which were washed three times with methanol to dehydrate the surface bound water molecules. The QDs are then stabilized in 5% solution of SHMP in chloroform with rigorous ultrasonication prior to spin coating. Since SHMP is a transparent oligomer matrix, the luminescence from the $\text{YVO}_4:\text{Eu}$ QDs remains unaffected and visibly brilliant. The SHMP capping retards the growth and agglomeration of QDs by preferentially nucleating onto the dangling bonds of the outermost O^- atoms of YVO_4 . By varying the molar ratio of $\text{YVO}_4:\text{Eu}$ QDs to the SHMP solution, the final particle density over the quartz substrate could be easily controlled. It has been observed that the structure and luminescent properties of the annealed nanophosphor layers are quite different from the bulk counterparts.¹³

Figure 1(a) shows the x-ray diffraction (XRD) profile of $\text{YVO}_4:\text{Eu}$ QDs corresponding to tetragonal zircon-type crystal structure.¹⁴ The broad XRD peaks are clear indications of the ultrafine nature of the particles. The average crystallite size was calculated to be ~ 5 nm using Scherer's formula.¹⁵ Superior optical transmittance ($\sim 80\%$ at 800 nm) and negligible scattering of light also indicate that the particles have almost zero dimensions. The inset of Fig. 1(a) shows a quartz cuvette containing colloidal solution of $\text{YVO}_4:\text{Eu}$ with minimum light scattering. Figure 1(b) shows the transmis-

^{a)}Electronic addresses: haranath@nplindia.org and haranath@mail.nplindia.ernet.in.

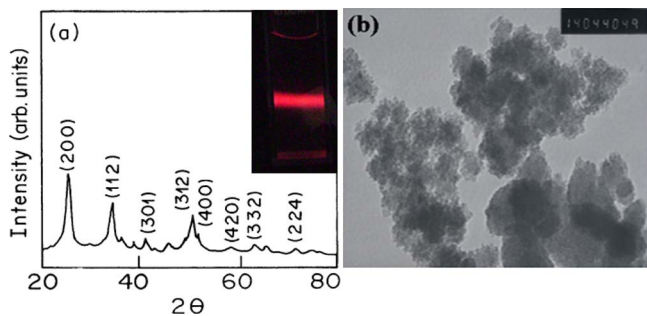


FIG. 1. (Color online) (a) XRD pattern of $\text{YVO}_4:\text{Eu}$ QDs. The inset shows the photograph of QD colloidal solution with no scattering of light. (b) TEM image (at magnification: 140 kX).

sion electron microscopy (TEM) image of the SHMP capped $\text{YVO}_4:\text{Eu}$ QDs with an average diameter of 3–5 nm ($\sigma = 0.2\text{--}0.4$). It is clearly seen that a very narrow size distribution of $\text{YVO}_4:\text{Eu}$ QDs with high order of stability and transparency has been achieved using the process employed. The conventional spin-coating method was used to dispense the $\text{YVO}_4:\text{Eu}$ QDs on a quartz substrate. One of the important prerequisites to ensure the uniform distribution of QDs is the cleanliness of the substrate. The quartz substrate was subjected to RCA cleaning and ultrasonication in acetone to ensure good adhesion for the QDs. For an easy control of the particle density on the surface the rotational speed of the spin coating was fixed at 1000 rpm and a number of coatings were optimized for $\sim 80\%$ transparency at 800 nm wavelength. The layers were then subjected to heat treatments up to 773 K for ~ 1 h to observe the modifications in the structural and luminescent properties. The annealing treatment also serves the basic purpose of removal of bounded organics, surface passivation of dangling bonds due to heat, and proper adhesion of the nanoparticles onto the quartz substrate.

Figure 2(a) shows the scanning electron microscopy (SEM) image of postannealed $\text{YVO}_4:\text{Eu}$ nanophosphor layer. Multiple coatings followed by heat treatment resulted in coalescence of QDs to form nanophosphor agglomerates of the order of 25 nm. A uniform distribution of particle aggregates is clearly seen throughout the surface in the SEM micrograph. Figure 2(b) shows the histogram of particle size distribution and relative packing density over the substrate. The average density of particles estimated from the micrograph was $\sim 4.2 \times 10^{10}$ particles/cm². The inset of Fig. 2(b) shows the representative photograph of a highly transparent ($\sim 80\%$ at 800 nm) and bright red-emitting $\text{YVO}_4:\text{Eu}$ nano-

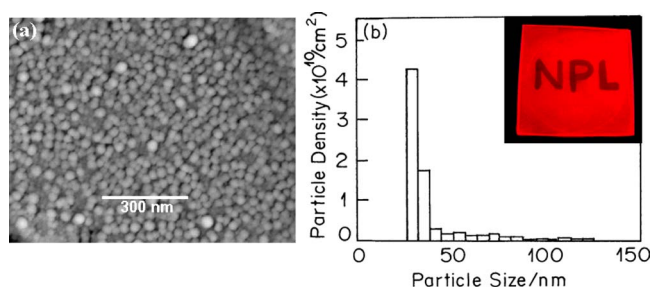


FIG. 2. (Color online) (a) SEM micrograph of annealed $\text{YVO}_4:\text{Eu}$ nanophosphor layer on quartz substrate and (b) particle density of the same layer as a function of particle size. The inset shows photograph of transparent bright red-emitting nanophosphor layer under 295 nm excitation.

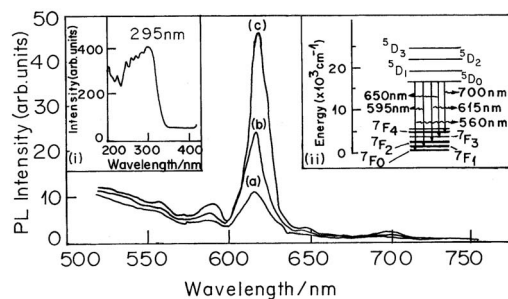


FIG. 3. Room temperature PL spectra of $\text{YVO}_4:\text{Eu}$ nanophosphor layer annealed at (a) 300 K, (b) 573 K, and (c) 773 K. Inset (i) shows broadband excitation spectrum and inset (ii) shows energy level diagram of Eu^{3+} .

phosphor layer after annealing. It is interesting to note that the particles do have excellent adhesion with narrow size distribution throughout the surface. This is one of the stringent requirements for the current industry dealing with photovoltaic cells and light emitting diodes. As per the industry's requirement, the particle densities were optimized for a minimum optical transparency of $\sim 80\%$ at 800 nm, which is far below the saturation density limit of the nanophosphor layer on quartz substrate. Below the saturation density the nanoparticles adhere strongly as transparent layers and for higher densities they tend to form localized three-dimensional clusters with local disorders and lose the transparency appreciably.

Figure 3 shows the room temperature PL spectra of $\text{YVO}_4:\text{Eu}$ coated layers heated at various temperatures to observe the annealing effects. Inset (i) in Fig. 3 shows the typical excitation spectrum of $\text{YVO}_4:\text{Eu}$ nanophosphor layer having a broadband absorption peak at ~ 295 nm, which is attributed to the sensitizing energy transfer state from the YVO_4 (host) to the Eu^{3+} (dopant). The broadband absorptions in the range of 225–280 nm are attributed to various intra- and intermolecular transitions of VO_4^{3-} in YVO_4 that are also contributing efficiently to the energy transfer mechanism.¹⁶ The characteristic emission bands observed at 560, 595, 615, 650, and 700 nm are due to efficient ${}^5D_0\text{--}{}^7F_J$ ($J=0\text{--}4$) Eu^{3+} transitions. The Eu^{3+} ions occupy Y^{3+} sites in YVO_4 crystal resulting in hypersensitive red emission at ~ 615 nm from ${}^5D_0\text{--}{}^7F_2$ transition, which is the most prominent emission in the PL spectra. Moreover, a moderate heating at 573 K improved the intensity of the PL peak while the peak position remained the same at ~ 615 nm. The effects became more prominent and saturated at and above 773 K. A slight blueshift in the PL emission peak as compared to that for the bulk- $\text{YVO}_4:\text{Eu}$ phosphor is attributed to the reduced dimensions and quantum confinement effects. The improvement in the PL intensity is mainly due to the axial compressive stress experienced by the bottom $\text{YVO}_4:\text{Eu}$ layer due to the layers above upon annealing. It has also been reported that the stress from the surface to the nanoparticle core slightly alters the lattice parameters.¹⁷ This in turn modifies the Eu^{3+} energy levels, as shown in inset (ii) of Fig. 3, to higher energy regions producing more efficient luminescence transition in terms of brighter, intense, and sharper PL peaks. Apart from this, effective surface passivation and dehydroxylation from the nanoparticles' surface are also reported to improve the PL characteristics.^{18,19} However, in the present case it is assumed that all these factors are contributing significantly to PL enhancement upon annealing. The layers

TABLE I. RH and temperature effects on PL intensity.

Sample No.	RH (%)	Temperature (°C)	PL intensity (arbitrary units)
1	12	75	1571
2	12	30	1924
3	50	30	1000
4	80	30	810

were subjected to various extreme relative humidity (RH) and temperature tests so as to observe their practical performance, and the result of such degradation study is shown in Table I. It can be seen that low (12%) RH and high temperature (~ 75 °C) conditions produce $\sim 36\%$ better PL intensity compared to ambient conditions, i.e., 50% RH and 30 °C. At same RH (i.e., 12%) and room temperature (~ 30 °C) conditions PL intensity increased further to $\sim 48\%$. High ($\sim 80\%$) RH and room temperature (30 °C) conditions decreased the PL intensity by $\sim 20\%$. The results suggest that low RH levels and ambient temperature conditions should be maintained in order to extract improved PL emissions from the nanophosphor layers.

Another interesting feature observed of the $\text{YVO}_4:\text{Eu}$ nanophosphor layer is the decrease in PL intensity after prolonged UV (254 nm) irradiation for about $\frac{1}{2}$ h. The PL intensity at 615 nm decreased to $\sim 25\%$ of its initial value. When a black paper mask covered a part of the nanophosphor layer during the UV irradiation, the covered part showed bright luminescence while the uncovered part did not. Moreover, the PL appearance and intensity regained almost the initial states after 24 h when stored up in dark conditions. Similar observations were made by Althues *et al.*²⁰ under inert and vacuum conditions that showed that the UV bleached parts did not recover. This indicates that oxygen plays a vital role in the regaining process of PL intensity. With this method, patterning of luminescent layer could be done, which may find application in developing volatile and nonvolatile optical data storage devices.

Time-resolved luminescence decay for $\text{YVO}_4:\text{Eu}$ nanophosphor layer was measured to investigate the dynamics of bound excitons. The decay was recorded for ${}^5D_0-{}^7F_2$ transition at 615 nm emission and 295 nm excitation by a time correlated single photon counting technique. The PL decay curve was measured with a xenon flash lamp as the source of excitation. Figure 4 clearly indicated that the luminescence lifetime for Eu^{3+} ions at 615 nm radiation was delayed for about 1038 μs . The lifetime data were very well fitted biex-

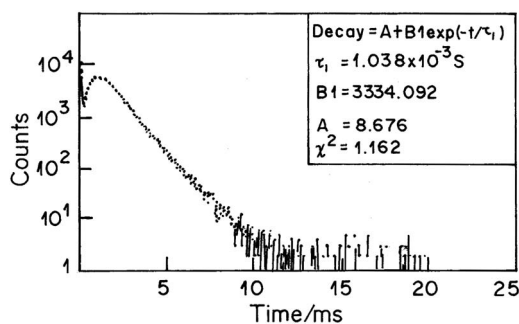


FIG. 4. Time-resolved PL decay spectrum of ${}^5D_0-{}^7F_2$ luminescence of Eu^{3+} in YVO_4 host at 300 K. The excitation energy is 295 nm (4.2 eV).

ponentially and the parameters generated from the fitting are listed in the inset of Fig. 4. The ${}^5D_0-{}^7F_2$ transition is an electric dipole transition and is quite sensitive to the surrounding of the Eu^{3+} ion.²¹ Since the transition occurs between the states of the same parity, the lifetime of the excited state is quite long. Moreover, the YVO_4 crystal structure has no inversion symmetry. Hence, the impediment experienced by the ${}^5D_0-{}^7F_2$ transition by a time constant of 1038 μs is attributed to electric dipole allowed and spin and parity forbidden transitions.^{22,23}

In summary, we have demonstrated a method for dispersing $\text{YVO}_4:\text{Eu}$ QDs as uniform 2D layers, which upon heat treatment coalesce to form nanoclusters with size of ~ 25 nm. The PL brightness of the layers increased many times and showed reversible photobleaching feature when exposed to high energy UV (254 nm) for more than 30 min. Due to significant quantum-size effects the absorption and emission peaks experienced a slight blueshift as compared to conventional bulk samples. Degradation studies conducted on 2D layer indicate that low RH and room temperature conditions would suit the best in improving the PL intensity substantially. The method presented of 2D layer deposition is promising and could be easily integrated to photovoltaic cells for better spectral response and energy conversion efficiency of the part of the solar spectrum.

The authors (A.F.K. and R.Y.) gratefully acknowledge the support from the Council of Scientific and Industrial Research (CSIR), India and Indian Institute of Technology Delhi (IIT-D) to work under research fellowship schemes.

¹H. Song and S. Lee, *Nanotechnology* **18**, 255202 (2007).

²P. Chung, H. Chung, and P. H. Holloway, *J. Vac. Sci. Technol. A* **25**, 61 (2007).

³T. Tsutsui, *Nature (London)* **420**, 752 (2002).

⁴X. Peng, J. Wickham, and A. P. Alivisatos, *J. Am. Chem. Soc.* **120**, 5343 (1998).

⁵S. Sun and C. B. Murray, *J. Appl. Phys.* **85**, 4325 (1999).

⁶V. F. Puentes, K. M. Krishnan, and A. P. Alivisatos, *Science* **291**, 2115 (2001).

⁷T. Igarashi, T. Isobe, and M. Senna, *Phys. Rev. B* **56**, 6444 (1997).

⁸R. N. Bhargava and D. Gallagher, *Phys. Rev. Lett.* **72**, 416 (1994).

⁹T. Sato, D. G. Hasko, and H. Ahmed, *J. Vac. Sci. Technol. B* **15**, 45 (1997).

¹⁰X. M. Lin, R. Parthasarathy, and H. M. Jaeger, *Appl. Phys. Lett.* **78**, 1915 (2001).

¹¹C. B. Murray, C. R. Kagan, and M. G. Bawendi, *Science* **270**, 1335 (1995).

¹²K. Riwozki and M. Haase, *J. Phys. Chem. B* **102**, 10129 (1998).

¹³D. Haranath, H. Chander, N. Bhalla, P. Sharma, and K. N. Sood, *Appl. Phys. Lett.* **86**, 201904 (2005).

¹⁴JCPDS Card No. 17-0341.

¹⁵B. D. Cullity, *Elements of X-Ray Diffraction*, 2nd ed. (Addison-Wesley, Reading, MA, 1978), p. 248.

¹⁶A. Huignard, T. Gacoïn, and J. P. Boilot, *Chem. Mater.* **12**, 1090 (2000).

¹⁷A. Bol, J. Ferwerda, J. Bergwerff, and A. Meijerink, *J. Lumin.* **99**, 325 (2002).

¹⁸W. Que, Y. Zhou, Y. Lam, Y. C. Chan, C. H. Kam, B. Liu, L. M. Gan, C. H. Chew, G. Q. Xu, S. J. Chua, S. J. Yu, and F. V. C. Mendis, *Appl. Phys. Lett.* **73**, 2727 (1998).

¹⁹B. Shen, T. Somaya, and Y. Arakawa, *Appl. Phys. Lett.* **76**, 2746 (2000).

²⁰H. Althues, P. Simon, and S. Kaskel, *J. Mater. Chem.* **17**, 758 (2007).

²¹X. Yang, S. Xiao, J. W. Ding, and X. H. Yan, *J. Appl. Phys.* **103**, 093101 (2008).

²²*Phosphor Handbook*, edited by S. Shionoya and W. M. Yen (CRC, New York, 1999), p. 244.

²³M. F. Bulanyi, V. I. Klimenko, A. V. Kovalenko, and B. A. Polezhaev, *Inorg. Mater.* **39**, 436 (2003).